Origin of Difference between One-Electron Redox Potentials of Guanosine and Guanine: Electrochemical and Quantum Chemical Study

Jan Langmaier,[†] Zdeněk Samec,*[,†] Eva Samcová,[‡] Pavel Hobza,*[,§] and David Řeha[§]

J. Heyrovský Institute of Physical Chemistry, Academy of Sciences of the Czech Republic, Dolejškova 3, 182 23 Prague 8, Czech Republic, Charles University, 3rd Faculty of Medicine, Center for Biomedical Sciences, Ruská 87, 100 00 Prague 10, Czech Republic, and Institute of Organic Chemistry and Biochemistry, Flemingovo nam. 2, 166 10 Prague 6, Czech Republic

Received: April 30, 2004; In Final Form: July 21, 2004

Cyclic voltammetry was used to measure the rates of the chemical oxidation of guanine (G), guanosine (Gs), 2′-deoxyguanosine (dG), and 2′-deoxyguanosine 5′-monophosphate (dGMP) by electrochemically generated tris(2,2′-bipyridyl)ruthenium(III). The numeric fit of voltammograms to an ECCCE type of mechanism provided the equilibrium and rate constants of the two-step chemical oxidation of the guanine species. One-electron redox potentials evaluated from the equilibrium constant of the first electron uptake follow the sequence G $<$ Gs $\approx$ dG $\approx$ dGMP, indicating that guanine is oxidized most easily. This sequence is expressed in the rate constant, which apparently follows the expected driving force dependence. Ab initio molecular orbital calculations were carried out using the DFT/B3LYP method with 6-31G** and 6-31++G** basis sets, and also the RI-MP2 method with the cc-pVDZ basis set, so as to clarify the role of various factors contributing to the redox potential. Theoretical results suggest that the difference between the one-electron redox potentials of Gs and G (ca. 0.13 V) originates partly from the higher energy of proton dissociation from the cation radical $Gs^{\bullet+}$ and partly from the higher difference in the hydration energy between the deprotonated radical $Gs(-H)^{\bullet}$ and the parent Gs, which compensate for the lower ionization potential of Gs compared to that of G.

Introduction

Guanine (G) is most easily oxidized of the nucleic acid bases, as indicated by the lowest values of ionization[1,2] and one-electron redox[3,4] potentials. The ionization potential of guanine is further lowered for stacked bases, e.g., GG[2,5] and GGG[6,7] sequences in DNA, which thus appear to be the sites of the specific DNA cleavage. These observations are of relevance to oxidative degradation of nucleic acids in mutagenesis, carcinogenesis, and aging.[8,9] Measurement of the electron-transfer equilibrium in solutions indicates that the redox potential of guanine depends also on the substitution at the N(9) site, e.g., for guanosine (Gs) it is by ca. 0.1 V more positive compared to that for G.[3] These results are supported by voltammetry of G and Gs oxidation at a graphite electrode.[10−13] Although the overall irreversibility of the electrode reaction and the adsorption effects preclude evaluating of the one-electron redox potentials, it is clear that Gs is oxidized at pH 7 at a potential by ca. 0.1 V more positive than G.[11] Apart from the computational method used, the substitution at the N(9) site can be responsible for the difference in the ionization potentials calculated for 9-methylG,[3] Gs,[5] and G.[14]

Both G[10−12] and Gs[11,12] undergo four-electron oxidation at a graphite electrode, leading to a series of products including guanidine, parabanic acid, and oxalyl guanidin.[10,13] Their identification[13] and the observed pH dependence of the half-wave potentials[10,11] lead the authors to propose a multistep mechanism initiated by concerted electron and proton uptake from the guanine moiety.[13] The intermediate formation of 8-oxo-7,8-dihydroguanine (8OG) was supposed to occur but was not proved, because 8OG is oxidized far more easily than the parent guanine base.[12] On the other hand, chemical oxidation of 2′-deoxyguanosine (dGs) in neutral aqueous solutions indicated that the product of the first electron transfer is uncharged,[8,15] i.e., the electron-transfer reaction is accompanied by a fast proton dissociation from N(1) of the radical cation $G^{\bullet+}$, $pK_a = 3.9$, to form the neutral radical $G(-H)^{\bullet}$.[15] The existence of proton-coupled electron transfer (PCET) from G is supported by kinetic studies of oxidation of mononucleotides[16,17] and single- and double-stranded DNA.[17] Several studies of the molecular mechanism point to a second electron-transfer step leading to 8OG.[18,19] A model with two-step guanine oxidation was used to simulate the catalytic oxidation of metal complexes, e.g., $Ru(bpy)_3^{2+}$ at an indium tin oxide (ITO) electrode,[20,21] though the contribution from the second electron transfer is likely to be as low as 1% or less.[22] Molecular calculations suggest that water addition to $G(-H)^{\bullet}$ on the C(8) site leading to 8OG is energetically much less favorable than in the case of $G^{\bullet+}$.[14] Hence, if 8OG were the intermediate of the pathway involving the neutral radical, the water addition to $G(-H)^{\bullet}$ should be preceded or concerted with the electron transfer.

In this paper, we propose an explanation for the difference between the one-electron oxidation−reduction (redox) potentials of G and Gs. First we shall employ the experimental approach and procedure[20−23] to evaluate the equilibrium constants and redox potentials for the first one-electron step in the oxidation of G, Gs, dGs, and 2′-deoxyguanosine 5′-monophosphate

* To whom correspondence may be addressed. E-mail: zdenek.samec@jh-inst.cas.cz. Fax: +420-286582307.
[†] Academy of Sciences of the Czech Republic.
[‡] Charles University.
[§] Institute of Organic Chemistry and Biochemistry.

10.1021/jp0481207 CCC: $27.50
Published on Web 09/15/2004

(dGMP) by electrochemically generated $Ru(bpy)_3^{3+}$. Second, we shall make a theoretical estimate of the difference in the redox potentials with the help of ab initio molecular orbital calculations to clarify the roles of various factors such as ionization potential, deprotonization, and hydration energy.

Experimental Section

Reagents. Guanine (2-amino-6-hydroxypurine), guanosine hydrate, 2′-deoxyguanosine hydrate, 2′-deoxyguanosine 5′-monophosphate disodium salt, 8-oxo-7,8-dihydro-2′-deoxyguanosine, tris(2,2′-bipyridyl)ruthenium(II) chloride hexahydrate, and the supporting electrolytes were purchased from Sigma-Aldrich. Aqueous solutions of the bases and of $Ru(bpy)_3Cl_2$ (bpy = 2,2′-bipyridine) in 1/15 M McIlvaine (pH 6.24) were prepared using highly purified and deionized water (Milli-Q, Millipore). Solutions were deoxygenated prior to measurements by argon bubbling.

Voltammetry and Digital Simulation. Voltammetric measurements were carried out in an all-glass cell by using a three-electrode potentiostat (Model 273A, EG&G PAR), which was equipped with an operating software (M270, EG&G PAR). F-doped tin oxide (FTO) coated-glass electrode (0.14 cm^2, Nippon Sheet Glass, 10 Ω/□) was cleaned following the same procedure as that used for an ITO electrode,[22] i.e., by sonification and washing with water and with supporting electrolyte solution prior to use. A Pt wire and an Ag|AgCl|sat. KCl electrode (0.197 V vs a saturated hydrogen electrode (SHE)) were used as the auxiliary and the reference electrode, respectively. All measurements were carried out at ambient temperature of 22 ± 2 °C.

Cyclic voltammograms were corrected for background current and fitted to an ECCCE type of mechanism consisting of a sequence of electrochemical (E) and chemical (C) reactions by using Digisim 3.03 software (BAS, USA). The mechanism was a modification of one adopted previously[20]

$$M^{3+} + e^- \leftrightarrows M^{2+} \quad (k_{el,M}{}^0, \alpha_M, E_M{}^0) \tag{1}$$

$$M^{3+} \leftrightarrows M^{2+} \quad (k_{f0}, K_0) \tag{2}$$

$$M^{3+} + G \leftrightarrows M^{2+} + G' \quad (k_{f1}, K_1) \tag{3}$$

$$M^{3+} + G' \leftrightarrows M^{2+} + G'' \quad (k_{f2}, K_2) \tag{4}$$

$$G'' \rightarrow P + e^- \ (k_{el,P}{}^0, \alpha_P, E_P{}^0) \tag{5}$$

where M represents the metal complex, $k_{el}{}^0$, α, and E are the standard rate constants, the apparent charge-transfer coefficients, and the standard redox potentials of the electrochemical reactions, respectively, and k_f and K are the forward rate and equilibrium constants of the chemical reactions, respectively. It can be reasonably assumed that the product G″ of the second electron transfer is 8OG, which is oxidized irreversibly at the FTO electrode in the potential range studied.[24] Therefore, we added the electrochemical step, eq 5, describing the one-electron oxidation of 8OG to a product P. Although the software employed allows optimizing the values of twelve parameters given in parentheses and six diffusion coefficients, the reliable determination of so many parameters in one fit is rather uncertain. Therefore, the parameters of electrochemical steps and the diffusion coefficients of species involved were fixed to the values found in the literature or determined in separate voltammetric experiments, vide infra. With reference to the results of polarographic measurements of adenine nucleotides and nucleosides,[25] the diffusion coefficients of all guanine species were fixed to 1×10^{-5} cm^2 s^{-1}. Each numeric fitting then provided the values of four parameters: k_{f1}, K_1, k_{f2}, and K_2.

Computational Methods. The molecular geometries of guanine and guanosine and their cation and neutral radicals were optimized using the DFT/B3LYP method with 6-31G** and 6-31++G** basis sets and also using a more reliable resolution of the identity MP2 (RI-MP2) method with the cc-pVDZ basis set. Ionization potentials of the neutral parent systems were determined as a difference between the energy of the parent (neutral) system and the respective cation radical (in both cases, the geometry was fully optimized). Deprotonization energies of cation radicals were calculated as a difference between the energies of cation radicals and deprotonated neutral radicals (again both geometries were fully optimized). Hydration-free energies of neutral parent systems and of the respective neutral deprotonated radical were obtained with self-consistent relaxation field method using the COSMO methodology (HF/6-31G*), as implemented in the Gaussian 03 suits of codes.[26] All other calculations were performed with Gaussian 03[26] and Turbomol[27,28] program packages.

Results and Discussion

Voltammetry of $Ru(bpy)_3^{2+}$ and 8OdGs. Cyclic voltammetry was used first to remeasure the parameters of the initial two steps in the reaction sequence, eqs 1 and 2. At sweep rates higher than 50 mV s^{-1}, the voltammetric behavior of $Ru(bpy)_3^{2+}$ can be simulated assuming a simple one-electron-transfer mechanism for the values of the parameters $k_{el,M}{}^0 = 0.1$ cm s^{-1}, $\alpha_M = 0.5$, and $E_M{}^0 = 1.06$ V. At lower sweep rates, the effect of conversion of the higher to lower oxidation state of the metal complex described by eq 2 is apparent, cf. inset A of Figure 1. A numeric fit of five cyclic voltammograms (CVs) of $Ru(bpy)_3^{2+}$ (5−100 mV/s) to an EC mechanism comprising the thermodynamically superfluous reaction (TSR), eq 2, yields the forward rate constant $k_{f0} = 0.044 \pm 0.006$ s^{-1}, the equilibrium constant $K_0 = 6 \times 10^7$, and the diffusion coefficients $D_{M^{3+}} = (6.6 \pm 1.1) \times 10^{-6}$ cm^2 s^{-1} and $D_{M^{2+}} = (4.3 \pm 0.4) \times 10^{-6}$ cm^2 s^{-1}, which agree well with literature data.[20,21,29] Voltammetric behavior of 8OdGs at FTO electrode was simulated to the simple E mechanism described by eq 5, which yields $k_{el,P}{}^0 = 5.7 \times 10^{-7}$ cm s^{-1}, $\alpha_P = 0.55$, $E_P{}^0 = 0.56$ V. In an agreement with the reported behavior on the ITO electrode,[30] the rate of Gs oxidation at the FTO electrode is far lower, cf. curves 1 and 2 in the inset B of Figure 1, and the contribution of the latter to the measured current was neglected.

Catalytic Electrochemistry. CVs of the $Ru(bpy)_3^{2+}$ oxidation in the presence of various guanine derivatives are shown in Figure 1. The measurements were performed for (a) 10 μM $Ru(bpy)_3^{2+}$ and four different concentrations of the guanine bases (20−100 μM) at the sweep rate of 10 mVs^{-1}, (b) 20 μM $Ru(bpy)_3^{2+}$ and 100 μM dGs at four different sweep rates (10−100 mV/s), and (c) six different concentrations of $Ru(bpy)_3^{2+}$ (10−60 μM) and 500 μM dGs at the sweep rate of 20 mV/s. The mean values of the rate and equilibrium constants obtained at various base concentrations are summarized in Table 1, cf. the caption for Figure 1. CV's simulated for these values agree well with those measured, cf. the solid and dashed lines in Figure 1. The results obtained for dGs are supported by measurements at various sweep rates yielding $k_{f1} = (2.4 \pm 1) \times 10^7$ M^{-1} s^{-1}, $K_1 = 13 \pm 6$, $k_{f2} = (3.8 \pm 2) \times 10^5$ M^{-1} s^{-1}, and $K_2 = (2.9 \pm 2) \times 10^{13}$ and by measurements at various concentrations of

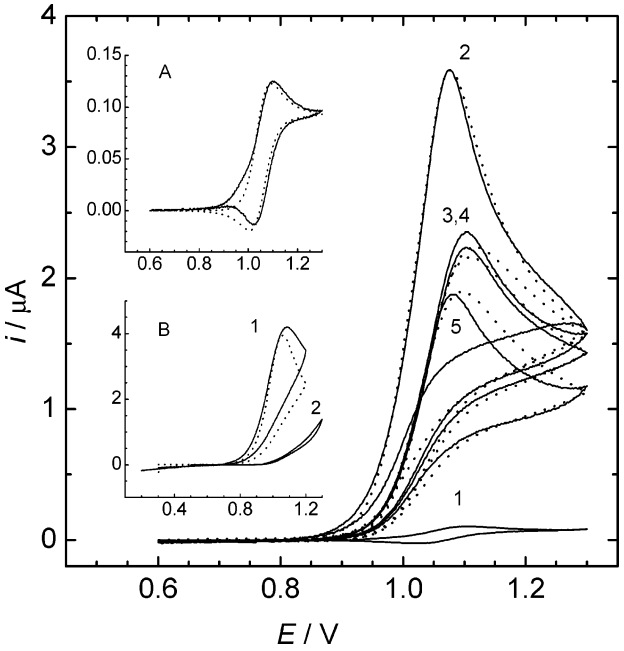

Figure 1. Cyclic voltammograms (solid lines) on a tin oxide coated-glass electrode (0.14 cm^2) at 10 mV/s and the numeric fit (dotted lines) for 10 μM $Ru(bpy)_3^{2+}$ in 1/15 M McIlvaine buffer (pH 6.24) in the absence (1) and presence (2−5) of 100 μM guanine base: (2) G (k_{f1} = 8.8 × 10^7 M^{-1} s^{-1}, K_1 = 7.9 × 10^3, k_{f2} = 1 × 10^6 M^{-1} s^{-1}, K_2 = 7.5 × 10^5); (3) dGs (k_{f1} = 7.8 × 10^6 M^{-1} s^{-1}, K_1 = 36, k_{f2} = 4 × 10^5 M^{-1} s^{-1}, K_2 = 10^{12}); (4) Gs (k_{f1} = 5.8 × 10^6 M^{-1} s^{-1}, K_1 = 52, k_{f2} = 3 × 10^5 M^{-1} s^{-1}, K_2 = 5 × 10^{11}); (5) dGMP (k_{f1} = 2 × 10^7 M^{-1} s^{-1}, K_1 = 28, k_{f2} = 3 × 10^5 M^{-1} s^{-1}, K_2 = 8 × 10^{12}). Insets: background-subtracted cyclic voltammograms (solid lines) and numeric fits (dotted lines) for (A) 20 μM $Ru(bpy)_3^{2+}$ at 5 mV s^{-1} and (B) 300 μM 8OdGs (curve 1) and 100 μM dGs (curve 2) at 20 mV s^{-1}, 1/15 M McIlvaine buffer (pH 6.24).

TABLE 1: Rate and Equilibrium Constants for Oxidation of Guanine Bases by $Ru(bpy)_3^{3+}$

base	$10^{-6}k_{f1}$ (M^{-1} s^{-1})	$10^{-1}K_1$	$E_1^{0\,a}$ (V)	$10^{-5}k_{f2}$ (M^{-1} s^{-1})	$10^{-12}K_2$
G	88 ± 14	790 ± 405	1.03	10 ± 6	(8 ± 4) × 10^{-7}
Gs	5 ± 2	4.8 ± 2	1.16	4 ± 1	1 ± 0.3
dGs	7 ± 4	2 ± 0.2	1.18	4 ± 2	29 ± 18
dGMP	13 ± 3	3.9 ± 2	1.17	3 ± 1	8 ± 3

[a] One-electron redox potentials (vs SHE) evaluated from K_1 using E_M^0 = 1.26 V.

the metal complex yielding k_{f1} = (2.8 ± 2) × 10^6 M^{-1} s^{-1}, K_1 = 14 ± 5, k_{f2} = (1.5 ± 0.5) × 10^5 M^{-1} s^{-1}, and K_2 = (5.4 ± 4) × 10^{12}.

These data point to an appreciable effect of the sugar moiety on the oxidation of guanine species. As it can be seen from Figure 1, guanine brings about the largest catalytic enhancement of the oxidation current, expressed in approximately 1 order of magnitude higher rate constant k_{f1} and in 2 orders of magnitude higher equilibrium constant K_1 for the first electron uptake compared to other guanine species. The difference in the rate constant between G and Gs, $RT\Delta \ln k_{f1}$ = 0.073 eV can be related to a higher driving force, $RT\Delta \ln K_1$ = 0.13 eV, which would correspond to the charge-transfer coefficient of 0.56. The driving force dependence of the rate constant k_{f1} for oxidation of guanine in calf thymus DNA by a series of metal complexes was investigated using catalytic electrochemistry[21] and stopped-flow spectrophotometry[17] yielding the charge-transfer coefficients of 0.49[21] and 0.8,[17] respectively. The latter value was considered to be evidence for the PCET mechanism.[17] There are few kinetic data published on the oxidation of isolated guanine species by $Ru(bpy)_3^{3+}$, e.g., the second-order rate constant for the faster reaction component of the oxidation of 2′-deoxyguanosine 5′-triphosphate (dGTP) was found to be 5.4 × 10^6 M^{-1} s^{-1}.[17] Fitting of the catalytic CV for guanosine 5′-triphosphate to the simple EC mechanism was not possible, while measurements of GMP provided k_{f1} = 6.4 × 10^5 M^{-1} s^{-1}.[30] However, the latter value was obtained assuming an unreliably low value for the diffusion coefficient of mononucleotides, 1.19 × 10^{-6} cm^2 s^{-1}.[30] Besides, we have found that simulation of the catalytic CVs of isolated guanine species requires including at least two following super-oxidation steps, such as those described by eqs 4 and 5. The ratio of the rate constants k_{f2}/k_{f1} falls in range 0.01−0.1, which is a result comparable with that for guanine oxidation in DNA.[22]

Table 1 also lists the values of the one-electron redox potentials E_1^0 obtained using the relationship

$$E_1^0 = E_M^0 + (RT/F) \ln K_1 \qquad (6)$$

where the standard redox potential for the $Ru(bpy)_3^{3+/2+}$ system E_M^0 = 1.06 V (vs Ag/AgCl), i.e., 1.26 V (vs SHE). The difference of 0.13 V between the redox potentials of G and Gs is corroborated by the results of chemical[3] or electrochemical[11] studies. The value of E_1^0 = 1.16 V for Gs is somewhat lower than the 1.29 ± 0.03 V (vs NHE) value obtained from the measured equilibrium constant of chemical oxidation of guanine in aqueous solution at pH 7.[4] Nevertheless, the former value is closer to the redox potential of guanine in double-helical DNA falling between 0.9 and 1.0 V vs Ag|AgCl at pH 7 (i.e., 1.10−1.20 V vs SHE), which was estimated on the basis of ability of metal complexes with different redox potentials to oxidize DNA.[23]

Theoretical Estimate of the Redox Potential. The first step in the oxidation of guanine species, eq 3, apparently proceeds as PCET.[15,17] Hence, the evaluated redox potential E_1^0 should have the physical meaning of standard potential for the electrode reaction

$$B(-H)^{\bullet} + H^+ + e^- \leftrightarrows B \qquad (7)$$

where B = G or Gs. With the help of a suitable Born−Haber cycle,[31] the redox potential can be then expressed as

$$E_1^0 = \frac{1}{F}(IP + DP + \Delta G^{hyd}) + \Delta E_1 \qquad (8)$$

where IP is the ionization potential of B, DP is the difference in energy between the deprotonated neutral radical $B(-H)^{\bullet}$ and the radical cation $B^{\bullet+}$, ΔG^{hyd} is the difference in the hydration free energies between $B(-H)^{\bullet}$ and B, and ΔE_1 comprises the constant energy terms associated with proton and electron.

The ionization potentials calculated at different theoretical levels for G and Gs are collected in Table 2. The data obtained for G are consistent with literature values calculated by using the DFT/B3LYP method.[14,32] It is evident that the largest IP values are obtained at the correlated level. However, irrespective of the theoretical level, IP for G is higher than that of Gs by up to 0.27 eV (RIMP2/cc-pVDZ), thus exhibiting an opposite change than E_1^0. On the other hand, the calculated DP values for G are systematically lower than those for Gs, both being largest again at the correlated level. It appears that the energy change due to the dissociation of proton presumably from N(1)[15] could compensate for the change in the ionization potential. Indeed, on passing from the B3LYP to the more reliable correlated level, the sum IP + DP becomes higher for Gs than

TABLE 2: Ionization Potentials, Deprotonization Energies, and Hydratation Free Energies for Guanine (G) and Guanosine (Gs) Determined at Three Theoretical Levels: (I) B3LYP/6-31G; (II) B3LYP/6-31++G**; (III) RIMP2/cc-pVDZ**

		energy/eV				
base	level	IP[a]	DP[b]	ΔG^{hyd} [c]	IP + DP	IP + DP + ΔG^{hyd}
G	I	7.32	10.59	0.13	17.91	18.04
	II	7.65	10.28		17.93	18.06
	III	7.88	10.65		18.53	18.66
Gs	I	7.18	10.68	0.19	17.86	18.05
	II	7.51	10.37		17.88	18.07
	III	7.61	11.09		18.70	18.89

[a] Difference between energies of cation radical and parent neutral system. [b] Difference between energies of deprotonated neutral radical and respective cation radical. [c] Difference in hydration-free energies between deprotonated neutral radical and parent neutral system.

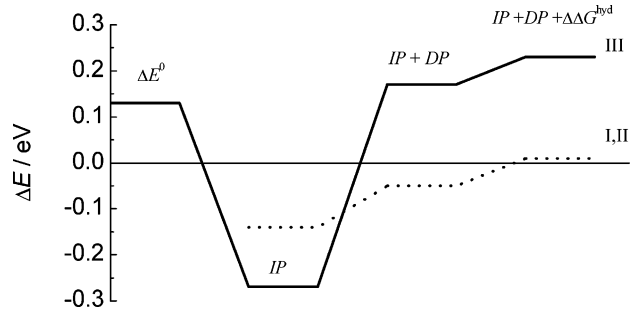

Figure 2. Comparison of the one-electron redox potential of Gs relative to G with the calculated difference in IP, the sum IP + DP and the sum IP + DP + ΔG^{hyd} at the B3LYP/6-31G** or B3LYP/6-31++G** level (dotted line) or the RIMP2/cc-pVDZ level (full line).

for G, cf. Figure 2, showing the diagram of energy changes. The difference ΔG^{hyd} in the hydration free energy between G(−H)• and G was found to exhibit a similar trend as DP, cf. Table 2. As it can be seen from the last column of Table 1, the inclusion of ΔG^{hyd} changes the order of total energies (IP + DP). Already at the simplest level (B3LYP/6-31G**) the difference between Gs and G becomes positive (0.01 eV), and when passing to the correlated value, it is significantly enlarged (0.23 eV) and it exceeds the difference in the one-electron redox potentials ($\Delta E_1^0 \approx 0.13$ V) at the correlated level, cf. Figure 2.

Conclusions

The sugar moiety has an appreciable effect on both the one-electron redox potential and the rate of oxidation of guanine species. Redox potentials for the first electron uptake follow the sequence G < Gs ≈ dG ≈ dGMP, indicating that guanine itself is oxidized most easily. This sequence is expressed in the rate constant, which apparently follows the expected driving force dependence. Ab initio molecular orbital calculations of the energy changes in PCET from Gs or G suggest that the difference between the one-electron redox potentials of Gs and G (ca. 0.13 V) originates partly from the higher energy of proton dissociation from the cation radical $Gs^{\bullet+}$ and partly from the higher difference in the hydration energy between the deprotonated radical Gs(−H)• and the parent Gs, which compensate for the lower ionization potential of Gs compared to that of G.

Acknowledgment. Financial support of this work by Grant Agency of the Czech Republic, Grant No. 203/01/0653, is gratefully acknowledged.

References and Notes

(1) Hush, N. S.; Cheung, A. S. *Chem. Phys. Lett.* **1975**, *34*, 11−13.
(2) Sugiyama, H.; Saito, I. *J. Am. Chem. Soc.* **1996**, *118*, 7063−7068.
(3) Jovanovic, S. V.; Simic, M. G. *J. Phys. Chem.* **1986**, *90*, 974−978.
(4) Steenken, S.; Jovanovic, S. V. *J. Am. Chem. Soc.* **1997**, *119*, 617−618.
(5) Prat, F.; Houk, K. N.; Foote, C. S. *J. Am. Chem. Soc.* **1998**, *120*, 845−846.
(6) Lewis, F. D.; Liu, X.; Liu. J.; Hayes, R. T.; Wasielewski, M. R. *J. Am. Chem. Soc.* **2000**, *122*, 12037−12038.
(7) (a) Nakatani, K.; Dohno, C.; Saito, I. *J. Am. Chem. Soc.* **2000**, *122*, 5893−5894. (b) Sistare, M. F.; Codden, S. J.; Heimlich, G.; Thorp, H. H. *J. Am. Chem. Soc.* **2000**, *122*, 4742−4749.
(8) Steenken, S. *Chem. Rev.* **1989**, *89*, 503−520.
(9) (a) Burrows, C. J.; Muller, J. G. *Chem. Rev.* **1998**, *98*, 1109−1151. (b) Kawanishi, S.; Hiraku, Y.; Oikawa, S. *Mutat. Rev.* **2001**, *488*, 65−76.
(10) Dryhurst, G.; Pace, G. *J. Electrochem. Soc.* **1970**, *117*, 1259−1264.
(11) Dryhurst, G. *Anal. Chim. Acta* **1971**, *57*, 137−149.
(12) Goyal, R. N.; Dryhurst, G. *J. Electroanal. Chem.* **1982**, *135*, 75−91.
(13) Subramanian, P.; Dryhurst, G. *J. Electroanal. Chem.* **1987**, *224*, 137−162.
(14) Reynisson, J.; Steenken, S. *Phys. Chem. Chem. Phys.* **2002**, *4*, 527−532.
(15) Candeias, L. P.; Steenken, S. *J. Am. Chem. Soc.* **1989**, *111*, 1094−1099.
(16) Shafirovich, V.; Dourandin, A.; Luneva, N. P.; Geacintov, N. E. *J. Phys. Chem. B* **2000**, *104*, 137.
(17) Weatherly; S. C.; Yang, I. V.; Thorp, H. H. *J. Am. Chem. Soc.* **2001**, *123*, 1236−1237.
(18) (a) Kino, K.; Saito, I.; Sugiyama, H. *J. Am. Chem. Soc.* **1998**, *120*, 7373−7374. (b) Duarte, V.; Muller, J. G.; Burrows, C. J. *Nucleic Acids Res.* **1999**, *27*, 496−502. (c) Doddridge, Z. A.; Cullis, P. M.; Jones, G. D. D.; Malone, M. E. *J. Am. Chem. Soc.* **1998**, *120*, 10998−10999.
(19) Choi, S.; Cooley, R. B.; Hakemian, A. S.; Larrabee, Y. C.; Bunt, R. C.; Maupas, S. D.; Muller, J. G.; Burrows, C. J. *J. Am. Chem. Soc.* **2004**, *126*, 591−598.
(20) Johnston, D. H.; Thorp, H. H. *J. Phys. Chem.* **1996**, *100*, 13837−13843.
(21) Johnston, D. H.; Glasgow, K. C.; Thorp, H. H. *J. Am. Chem. Soc.* **1995**, *117*, 8933−8938.
(22) Sistare, M. F.; Holmberg, R. C.; Thorp, H. H. *J. Phys. Chem. B* **1999**, *103*, 10718−10728.
(23) Johnston, D. H.; Cheng, C.-C.; Campbell, K. J.; Thorp, H. H. *Inorg. Chem.* **1994**, *33*, 6388−6390.
(24) Langmaier, J.; Samec, Z.; Samcová, E. *Electroanalysis* **2003**, *15*, 1555−1560.
(25) Janik, B.; Elving, P. J. *J. Am. Chem. Soc.* **1970**, *92*, 235−243.
(26) Frisch, M. J.; Trucks, G. W.; Schlegel, H. B.; Scuseria, G. E.; Robb, M. A.; Cheeseman, J. R.; Montgomery, J. A., Jr.; Vreven, T.; Kudin, K. N.; Burant, J. C.; Millam, J. M.; Iyengar, S. S.; Tomasi, J.; Barone, V.; Mennucci, B.; Cossi, M.; Scalmani, G.; Rega, N.; Petersson, G. A.; Nakatsuji, H.; Hada, M.; Ehara, M.; Toyota, K.; Fukuda, R.; Hasegawa, J.; Ishida, M.; Nakajima, T.; Honda, Y.; Kitao, O.; Nakai, H.; Klene, M.; Li, X.; Knox, J. E.; Hratchian, H. P.; Cross, J. B.; Adamo, C.; Jaramillo, J.; Gomperts, R.; Stratmann, R. E.; Yazyev, O.; Austin, A. J.; Cammi, R.; Pomelli, C.; Ochterski, J. W.; Ayala, P. Y.; Morokuma, K.; Voth, G. A.; Salvador, P.; Dannenberg, J. J.; Zakrzewski, V. G.; Dapprich, S.; Daniels, A. D.; Strain, M. C.; Farkas, O.; Malick, D. K.; Rabuck, A. D.; Raghavachari, K.; Foresman, J. B.; Ortiz, J. V.; Cui, Q.; Baboul, A. G.; Clifford, S.; Cioslowski, J.; Stefanov, B. B.; Liu, G.; Liashenko, A.; Piskorz, P.; Komaromi, I.; Martin, R. L.; Fox, D. J.; Keith, T.; Al-Laham, M. A.; Peng, C. Y.; Nanayakkara, A.; Challacombe, M.; Gill, P. M. W.; Johnson, B.; Chen, W.; Wong, M. W.; Gonzalez, C.; Pople, J. A. *Gaussian 03*, revision B.02; Gaussian, Inc.: Pittsburgh, PA, 2003.
(27) Ahlrichs, R.; Bar, M.; Haser, M.; Ehring, M.; Kolmel, C. *Chem. Phys. Lett.* **1989**, *162*, 165.
(28) Weigend, F.; Haser, M. *Theor. Chem. Acc.* **1997**, *97*, 331.
(29) Creutz, J.; Sutin, N. *Proc. Natl. Acad. Sci. U. S. A.* **1975**, *72*, 2858−2862.
(30) Kim, J. *Bull. Korean Chem. Soc.* **2000**, *21*, 709−711.
(31) Trasatti, S. *Pure Appl. Chem.* **1986**, *58*, 955−966.
(32) Wetmore, S. D.; Boyd, R. J.; Eriksson, L. A. *J. Phys. Chem. B*, **1998**, *102*, 9332−9343.